Charge states of vacancies in germanium investigated by simultaneous observation of germanium self-diffusion and arsenic diffusion

Miki Naganawa,[1,a)] Yasuo Shimizu,[1] Masashi Uematsu,[1] Kohei M. Itoh,[1,b)] Kentarou Sawano,[2] Yasuhiro Shiraki,[2] and Eugene E. Haller[3]
[1]*Department of Applied Physics and Physico-Informatics, Keio University, 3-14-1 Hiyoshi, Kohoku-ku, Yokohama 223-8522, Japan*
[2]*Research Center for Silicon Nano-Science, Advanced Research Laboratories, Musashi Institute of Technology, 8-15-1 Todoroki, Setagaya-ku, Tokyo 158-0082, Japan*
[3]*University of California at Berkeley and Lawrence Berkeley National Laboratory, 1 Cyclotron Road, Berkeley, California 94720, USA*

(Received 10 October 2008; accepted 23 October 2008; published online 11 November 2008)

Diffusion of germanium (Ge) and arsenic (As) has been investigated simultaneously using As-implanted Ge isotope superlattices. No transient enhanced diffusion of As that could have arisen by the implantation damage is observed. A quadratic dependence of the Ge self-diffusion on the carrier concentration due to the Fermi level effect is observed. A precise reproduction of the Ge and As diffusion profiles by a numerical simulator lets us conclude that doubly negatively charged vacancies are the dominant point defects responsible for more than 95% of the self-diffusion in intrinsic Ge and this fraction increases even further in *n*-type Ge. © *2008 American Institute of Physics*. [DOI: 10.1063/1.3025892]

The recent growth in interest in germanium (Ge) FETs has encouraged researchers to revisit fundamental studies of impurities in Ge.[1–3] Among many impurities, arsenic (As) is one of the most important dopants for the fabrication of shallow junctions for the *n*-channel devices. However, our level of understanding of the diffusion mechanisms in Ge is much less advanced than that in silicon (Si). For example, while Ge self-diffusion has been known to occur via the vacancy mechanism,[4–6] whether transient enhanced diffusion (TED) due to implantation damage does exist or not, has not been clarified yet. Quite recently, Brotzmann *et al.*[5] determined the charge state of vacancies in Ge by the simultaneous observation of Ge self-diffusion and *n*-dopant diffusion in natural Ge (^{nat}Ge) and seventy Ge (^{70}Ge) isotope multilayer structures whose ^{70}Ge layers were doped with carbon (C) ($>10^{19}$ cm^{-3}), whereas the C concentration of the adjacent ^{nat}Ge layers was below the detection limit of secondary ion mass spectrometry (SIMS). From the Ge self-diffusion in regions of both very low and high C concentrations, they concluded that the Ge vacancy was doubly negatively charged and that the self-diffusion was not affected by the presence of C even though the diffusion of donors was affected by the high concentration of C. In this report, we performed diffusion studies under intrinsic and extrinsic As doping conditions using Ge isotope superlattices (SLs) whose C concentration is below 1×10^{17} cm^{-3}. In order to probe the charge states of vacancies in Ge, we simultaneously measured Ge self-diffusion and As diffusion using the Ge isotope SLs and simulated the diffusion profiles. We confirm in the findings of Brotzmann *et al.* that negatively charged vacancies are the dominant point defects responsible for the self-diffusion in Ge and deduce the fraction of the doubly negatively charged vacancies.

Samples employed in this study were prepared as follows. Ge isotope SLs with alternating layers of ^{nat}Ge and ^{70}Ge were fabricated by solid-source molecular beam epitaxy.[7,8] On top of the 2 in. Ge (100) wafers, a ^{nat}Ge buffer layer was grown to achieve an atomically flat, smooth surface. Then, the alternating layers of isotopically enriched ^{70}Ge (^{70}Ge:96.3%, ^{74}Ge:0.2%) and ^{nat}Ge (^{70}Ge:20.5%, ^{74}Ge:36.5%) were grown. The thickness of each isotope layer was 15 nm. The total thickness of the Ge isotope SLs was chosen so that As diffuses through the entire structure within a reasonable combination of time and temperature. Additionally, a ^{nat}Ge cap layer was grown on the top of the isotope multilayer structure. The C concentration in the sample was below the detection limit of SIMS (PHI Adept1010) ($<1\times10^{17}$ cm^{-3}). ^{75}As^{+} ions were implanted at room temperature into the ^{nat}Ge cap layer of the samples so that the Ge isotope SLs were not perturbed by the implantation. The implantation energy was 90 keV, and As doses were 2×10^{13} and 2×10^{14} cm^{-2} to make the samples at the diffusion temperature intrinsic and extrinsic, respectively. After the implantation, the wafers were cut into 2.5 $\times$2.5 mm^2 pieces and diffusion annealed at 450–550 °C for 1–48 h in a resistively heated furnace. The samples were placed face to face with As-doped Ge substrates in order to avoid As loss during annealing. A semiconductor-processing-grade quartz tube was employed for keeping the sample as clean as possible. Diffusion annealing was conducted under flowing 99.999% pure Ar at a rate of 1.2 l/min. The depth profiles of Ge and As were determined by SIMS. Primary ions used for the profiling of ^{74}Ge and ^{75}As were Cs^{+} with the acceleration energy of 2 keV.

We simulated Ge self-diffusion and As diffusion profiles according to the vacancy mechanism described below. Contributions of both doubly and singly negatively charged vacancies (V^{2-} and V^{-}) were taken into account by the following reactions:

$$(AsV)^{-} \Leftrightarrow As_s^{+} + V^{2-},$$

a)Electronic mail: naganawa@a8.keio.jp.
b)Electronic mail: kitoh@appi.keio.ac.jp.

$$^{74}V^{2-} \Leftrightarrow {}^{74}\mathrm{Ge}_s + V^{2-},$$

$$(\mathrm{As}V)^- \Leftrightarrow \mathrm{As}_s^+ + V^- + e,$$

$$^{74}V^- \Leftrightarrow {}^{74}\mathrm{Ge}_s + V^-, \quad (1)$$

where e denotes an electron. The first and third reactions describe As diffusion via V^{2-} and V^-, respectively. $(\mathrm{As}V)^-$ denotes the nearest-neighbor pair configuration in which As_s^+ (substitutional, ionized As) becomes mobile through site exchange with vacancies. The As diffusivity in Ge is proportional to the square of the As concentration, which shows that the charge of the pair is singly negative.[9] The second and fourth reactions describe Ge self-diffusion via V^{2-} and V^-, respectively. These reactions lead to the following set of coupled partial differential equations:

$$\frac{\partial C_s}{\partial t} = G_1 + G_3,$$

$$\frac{\partial C_{v^-}}{\partial t} = \frac{\partial}{\partial x}\left(D_{v^-}\frac{\partial C_{v^-}}{\partial x} - D_{v^-}\frac{C_{v^-}}{n}\frac{\partial n}{\partial x}\right) - G_1 - G_3,$$

$$\frac{\partial C_{^{74}\mathrm{Ge}_s}}{\partial t} = G_2 + G_4,$$

$$\frac{\partial C_{^{74}V^{2-}}}{\partial t} = \frac{\partial}{\partial x}\left(D_{^{74}V^{2-}}\frac{\partial C_{^{74}V^{2-}}}{\partial x} - 2D_{^{74}V^{2-}}\frac{C_{^{74}V^{2-}}}{n}\frac{\partial n}{\partial x}\right) - G_2,$$

$$\frac{\partial C_{V^{2-}}}{\partial t} = \frac{\partial}{\partial x}\left(D_{V^{2-}}\frac{\partial C_{V^{2-}}}{\partial x} - 2D_{V^{2-}}\frac{C_{V^{2-}}}{n}\frac{\partial n}{\partial x}\right) + G_1 + G_2,$$

$$\frac{\partial C_{^{74}V^-}}{\partial t} = \frac{\partial}{\partial x}\left(D_{^{74}V^-}\frac{\partial C_{^{74}V^-}}{\partial x} - D_{^{74}V^-}\frac{C_{^{74}V^-}}{n}\frac{\partial n}{\partial x}\right) - G_4,$$

$$\frac{\partial C_{V^-}}{\partial t} = \frac{\partial}{\partial x}\left(D_{V^-}\frac{\partial C_{V^-}}{\partial x} - D_{V^-}\frac{C_{V^-}}{n}\frac{\partial n}{\partial x}\right) + G_3 + G_4, \quad (2)$$

where G_1-G_4, respectively, denote the generation terms for reactions (2) such that

$$G_1 = k_{1f}C_{v^-} - k_{1b}C_sC_{V^{2-}},$$

$$G_2 = k_{2f}C_{^{74}V^{2-}} - k_{2b}C_{^{74}\mathrm{Ge}_s}C_{V^{2-}},$$

$$G_3 = k_{3f}C_{v^-} - k_{3b}C_sC_{V^-}n,$$

$$G_4 = k_{4f}C_{^{74}V^-} - k_{4b}C_{^{74}\mathrm{Ge}_s}C_{V^-}. \quad (3)$$

In Eqs. (2) and (3), C_x ($x=v^-$, s, $^{74}\mathrm{Ge}_s$, $^{74}V^{2-}$, $^{74}V^-$, V^{2-}, and V^-, respectively, for $(\mathrm{As}V)^-$, As_s^+, $^{74}\mathrm{Ge}_s$, $^{74}V^{2-}$, $^{74}V^-$, V^{2-}, and V^-) is the concentration of x, D_x is the diffusivity of x, n is the electron concentration, and k_m is the rate constant of the mth reaction in Eq. (3) ($m=1-4$), with f and b denoting forward and backward reactions. In Eqs. (1)–(3), $^{74}V^{2-}$ and $^{74}V^-$ denote the configurations in which $^{74}\mathrm{Ge}_s$ becomes mobile through site exchange with V^{2-} and V^-, in a similar manner to $(\mathrm{As}V)^-$, and the same diffusivity was used for $^{74}V^{2-}$ and V^{2-} (and for $^{74}V^-$ and V^-). Equation (2) was solved numerically using the partial differential equation solver ZOMBIE (Ref. 10) to simulate the simultaneous Ge self-diffusion and As diffusion profiles. The intrinsic carrier concentration used for simulation was obtained from $np=3.10\times10^{32}T^3\exp(-0.785/kT)$.[11] Note that only the V^{2-} contribution in Eq. (1) was taken into account in the simulation employed below unless otherwise stated.

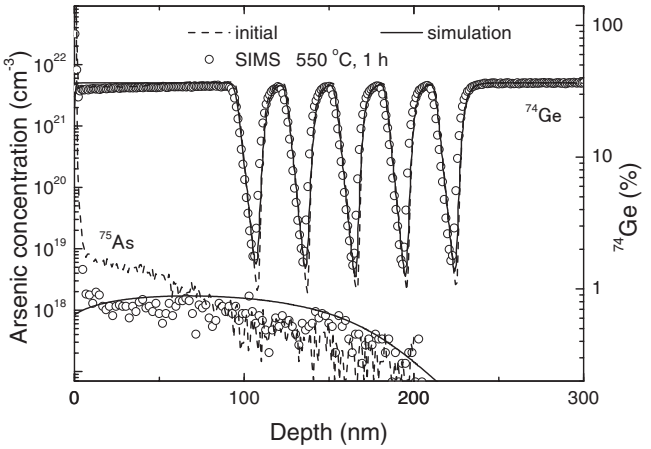

FIG. 1. SIMS and simulated depth profiles of ^{74}Ge (upper profiles) and ^{75}As (lower profiles) in the ^{nat}Ge/^{70}Ge isotope SLs implanted with $^{75}As^+$ at 90 keV, 2×10^{13} cm^{-2}. In both the upper and the lower profiles, broken lines and open circles represent the SIMS profiles before and after annealing at 550 °C for 1 h, respectively. Solid curves are the simulation results.

Figure 1 shows the SIMS and simulated depth profiles of ^{74}Ge and ^{75}As before and after 1 h annealing at 550 °C for the samples whose As dose is 2×10^{13} cm^{-2}. For this dose, Ge diffusion and As diffusion proceed under intrinsic condition because the concentration of As is kept below the intrinsic carrier concentrations at the diffusion-annealing temperatures covered in this study. Prior to the present study, the same Ge isotope SL without As implantation was employed to measure the intrinsic Ge self-diffusivity to confirm the excellent agreement with the previously reported Ge self-diffusivity for thermal equilibrium.[4] This self-diffusivity was used for the simulation of the Ge diffusion profiles of As-implanted samples shown in Fig. 1. In addition, the As profiles were fitted using the intrinsic As diffusivity as a parameter, and the diffusivity obtained agreed well with the previous values determined for the thermal equilibrium.[9] The solid lines in Fig. 1 represent the calculated diffusion profiles of Ge and As using the thermal intrinsic Ge self-diffusivity and As diffusivity described above.

Figures 2 and 3 show the SIMS and simulated depth profiles of ^{74}Ge and ^{75}As before and after annealing at 550 °C for 1 h (Fig. 2) and at 500 °C for 3 and 6 h (Fig. 3) for the samples whose As implant dose is 2×10^{14} cm^{-2}. In this case, the diffusion takes place under extrinsic conditions and therefore diffusion of As is enhanced in the high concentration region, leading to a box-shape profile.[12] In Fig. 2, the calculated diffusion profiles (solid curves) using the same values of the thermal intrinsic Ge self-diffusivity and As diffusivity as for Fig. 1 reproduce the experimental profiles very well. In addition, the experimental profiles in Fig. 3 are well reproduced by using the values of the thermal intrinsic Ge self-diffusivity[4] and As diffusivity[9] at 500 °C. This indicates that TED was not present under the experimental conditions employed in this study because the thermal Ge self-diffusivity and As diffusivity were used exclusively in the calculation. The absence of TED is quite different from the

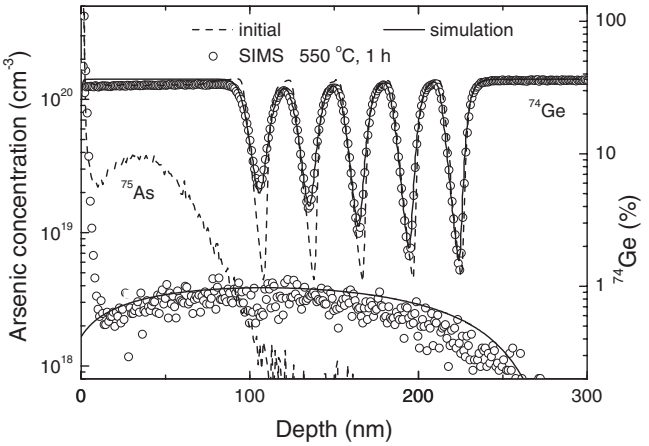

FIG. 2. SIMS and simulated depth profiles of ^{74}Ge (upper profiles) and ^{75}As (lower profiles) in the ^{nat}Ge/^{70}Ge isotope SLs implanted with $^{75}As^{+}$ at 90 keV, 2×10^{14} cm^{-2}. In both the upper and the lower profiles, broken lines and open circles represent the SIMS profiles before and after annealing at 550 °C for 1 h, respectively. Solid curves are the simulation results.

diffusion in implanted Si, where the diffusion is time dependent and enhanced significantly by implantation-induced damage forming {311} Si self-interstitial clusters.[13,14] In our study, the diffusion was found to be in thermal equilibrium and no time dependence was observed for As implanted into Ge, whose dose would be high enough to induce TED in Si. At present, isolated Ge self-interstitials have not been observed, although interstitial-type {311} defects have been found after hydrogen implantation in Ge.[15] Because self-interstitials would be related to TED, additional efforts are required to investigate the existence of the self-interstitial atoms and related defects in Ge.

The precise reproduction of the Ge diffusion profiles in Figs. 2 and 3 based on our model means that Ge self-diffusivity shows a quadratic dependence on the carrier concentration. This confirms the previous report[5] that V^{2-} is the dominant point defect that governs the diffusion in Ge. Moreover, in order to precisely determine the contributions

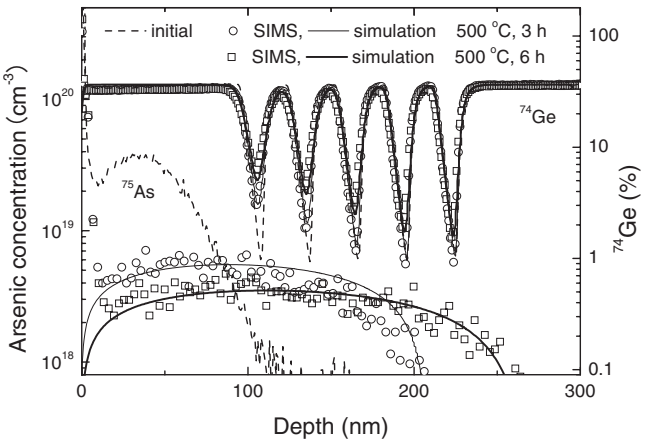

FIG. 3. SIMS and simulated depth profiles of ^{74}Ge (upper profiles) and ^{75}As (lower profiles) in the ^{nat}Ge/^{70}Ge isotope SLs implanted with $^{75}As^{+}$ at 90 keV, 2×10^{14} cm^{-2}. In both the upper and the lower profiles, broken lines, open circles, and open squares represent the SIMS profiles before and after annealing at 500 °C for 3 and 6 h, respectively. Solid curves are the simulation results.

of V^{2-} and V^{-} to the self-diffusion, we employed the calculation that takes into account both V^{2-} and V^{-}. In the calculation, the fractions of V^{2-} and V^{-} were changed but the sum of two contributions was kept equal to the intrinsic Ge self-diffusivity. When the fraction of V^{2-} was smaller than 0.95 (i.e., that of V^{-} is larger than 0.05), the calculation underestimated the experimental results. This indicates that the contribution of V^{2-} under intrinsic conditions is larger than 95% and that of V^{-} is quite minor. This fraction increases even further in *n*-type Ge due to the Fermi level effect. This means that V^{2-} is a dominant point defect in intrinsic and *n*-type Ge. Note that the contribution of neutral vacancies (V^{0}) should be smaller than that of V^{-} because an introduction of the V^{0} contribution would further underestimate the Ge self-diffusion.

In summary, the charge states of vacancies in Ge have been determined by simultaneous observation of Ge self-diffusion and As diffusion using As-implanted Ge isotope SLs. TED due to the implantation damages was not observed in this study. Under extrinsic conditions, a quadratic dependence of the Ge self-diffusivity on the carrier concentration has been obtained. We confirm that V^{2-} is the dominant point defect for the diffusion in Ge. In addition, we have identified the contribution of V^{2-} under intrinsic conditions to be larger than 95% and this fraction increases even further in *n*-type Ge due to the Fermi level effect. We believe that the incorporation of our findings to process simulators is necessary for the development of shallow junctions in Ge-based FETs.

This work has been supported in part by the Research Program on Collaborative Development of Innovative Seeds by JST, in part by Special Coordination Funds for Promoting Science and Technology for INQIE, and in part by Keio Global COE Program.

[1] A. Chroneos, H. Bracht, R. W. Grimes, and B. P. Uberuaga, Appl. Phys. Lett. **92**, 172103 (2008).
[2] M. Koike, Y. Kamata, T. Ino, D. Hagishima, K. Tatsumura, M. Koyama, and A. Nishiyama, J. Appl. Phys. **104**, 023523 (2008).
[3] S. Mirabella, G. Impellizzeri, A. M. Piro, E. Bruno, and M. G. Grimaldi, Appl. Phys. Lett. **92**, 251909 (2008).
[4] M. Werner, H. Mehrer, and H. D. Hochheimer, Phys. Rev. B **32**, 3930 (1985).
[5] S. Brotzmann, H. Bracht, J. Lundsgaard Hansen, A. Nylandsted Larsen, E. Simoen, E. E. Haller, J. S. Christensen, and P. Werner, Phys. Rev. B **77**, 235207 (2008).
[6] A. Chroneos, R. W. Grimes, B. P. Uberuaga, and H. Bracht, Phys. Rev. B **77**, 235208 (2008).
[7] K. Itoh, W. L. Hansen, E. E. Haller, J. W. Farmer, V. I. Ozhogin, A. Rudnev, and A. Tikhomirov, J. Mater. Res. **8**, 1341 (1993).
[8] K. Morita, K. M. Itoh, J. Muto, K. Mizoguchi, N. Usami, Y. Shiraki, and E. E. Haller, Thin Solid Films **369**, 405 (2000).
[9] S. Brotzmann and H. Bracht, J. Appl. Phys. **103**, 033508 (2008).
[10] W. Jüngling, P. Pichler, S. Selberherr, E. Guerrero, and H. W. Pötzl, IEEE Trans. Electron Devices **ED-32**, 156 (1985).
[11] F. J. Morin and J. P. Maita, Phys. Rev. **94**, 1525 (1954).
[12] H. Bracht and S. Brotzmann, Mater. Sci. Semicond. Process. **9**, 471 (2006).
[13] D. J. Eaglesham, P. A. Stolk, H.-J. Gossmann, and J. M. Poate, Appl. Phys. Lett. **65**, 2305 (1994).
[14] L. Pelaz, G. H. Gilmer, V. C. Venezia, H.-J. Gossmann, M. Jaraiz, and J. Barbolla, Appl. Phys. Lett. **74**, 2017 (1999).
[15] M. L. David, F. Pailloux, D. Babonneau, M. Drouet, J. F. Barbot, E. Simoen, and C. Claeys, J. Appl. Phys. **102**, 096101 (2007).